Journal of Nuclear Materials 408 (2011) 116–124

Contents lists available at ScienceDirect

Journal of Nuclear Materials

journal homepage: www.elsevier.com/locate/jnucmat

Microstructural influence on high temperature creep flow of Zr–1%NbO alloy in near-α, (α + β), and β temperature ranges in a high vacuum environment

Djilali Kaddour [a,1], Anne-Françoise Gourgues-Lorenzon [a,*], Jean-Christophe Brachet [b], Laurence Portier [b], André Pineau [a]

[a] MINES ParisTech, Centre des Matériaux, CNRS UMR 7633, B.P. 87, 91003 Evry cedex, France
[b] CEA, DEN, Serv. Rech. Met. Appl., 91191 Gif-sur-Yvette, France

ARTICLE INFO

Article history:
Received 27 July 2010
Accepted 11 November 2010

ABSTRACT

Uniaxial tensile creep tests were carried out at 650–1100 °C in a high vacuum environment on Zr–1%NbO tubes with various microstructures. The effect of microstructure on creep flow in the (α + β) temperature range is significant (the creep rate being modified by up to three orders of magnitude) under stresses lower than 10 MPa, that is, for stress values of one order of magnitude lower than those characteristic of prototypical Loss-of-coolant-accident (LOCA) conditions. Under stresses higher than about 20 MPa, this effect is much smaller. No transformation-induced plasticity was detected from anisothermal creep tests, once the creep strain was thoroughly taken into account to process experimental strain vs. time data.

1. Introduction

This paper is devoted to describe the relationships between microstructure and creep properties of a zirconium–niobium alloy in a wide range of temperatures and strain rates involving both high temperature (β, bcc) and low-temperature (α, hcp) phases. Zirconium-based alloys are currently used as cladding tubes in the fuel assembly of nuclear light water reactors. Although the normal operating temperature is lower than 400 °C (i.e., well within the α phase domain), one must ensure integrity and avoid excess ballooning of cladding tubes up to high temperatures and for high (internal pressure) stresses under Loss-of-coolant-accident (LOCA) conditions. Such a hypothetical accidental scenario involves high temperature cycles (up to the temperature range for which the β phase is stable) in an oxidising (steam) environment. The present study aims at understanding the contribution of the metallurgical state of the zirconium-based alloy to the high temperature behaviour, without taking significant hardening of the material (due to rapid oxidation at high temperature) into account. Thus, all creep tests were performed under a high vacuum and applied (tensile) stresses are of one order of magnitude lower than stresses typical of hypothetical LOCA transients.

A Zr–1%NbO alloy was chosen. Due to its niobium content, it is possible to "quench" the high temperature β phase by transforming it into an acicular product, typical of the on-cooling β to α phase transformation, namely, "colonies" with plate-shaped α grains separated by some retained Nb-enriched β films and/or stringers, the volume fraction of this metastable β phase being less than a few percents. These "colonies", which will be denoted as "prior-β" in the following, can easily be distinguished from the primary (equiaxed) α phase, which did not transform into β at high temperature. Thus, information about the high temperature microstructure may be obtained after rapid cooling of specimens after the tests. In addition, several creep regimes may be investigated within a reasonable time, as this alloy exhibits no significant sensitivity to the loading history for the stress and temperature ranges investigated in this study.

Creep data have already been reviewed for pure zirconium [1], and for zirconium-based alloys [2–4] in a wide temperature range. The purpose of the present paper is two-fold:

- Improving understanding of interactions between creep and microstructure of Zr-based alloys in the near-α and (α + β) temperature ranges.
- Improving understanding of the complex creep behaviour of Zr-based alloys in the (α + β) temperature range.

For this purpose, creep tests were carried out by using specimens with various « model » microstructures, which were produced after laboratory heat treatments designed for that purpose. Here, the "microstructure" of the considered specimens is considered at the grain level, but does not explicitly consider the

* Corresponding author. Tel.: +33 1 60 76 30 66; fax: +33 1 60 76 31 50.
E-mail addresses: djilali.kaddour@areva.com (D. Kaddour), anne-francoise.gourgues@mines-paristech.fr (A.-F. Gourgues-Lorenzon), jean-christophe.brachet@cea.fr (J.-C. Brachet), laurence.portier@cea.fr (L. Portier), andre.pineau@mines-paristech.fr (A. Pineau).
[1] Present address: AREVA NP, NEEMFT, Materials, Technology and Chemistry Department, Tour AREVA, 1, Place Jean Millier, 92084 Paris La Défense cedex, France.

0022-3115/$ - see front matter © 2010 Elsevier B.V. All rights reserved.
doi:10.1016/j.jnucmat.2010.11.025

dislocation structure (which may yet differ between equiaxed and colony-shaped α phases) and the precipitation state (as Fe and Cr-rich precipitates are dissolved at most of the test temperatures considered here).

As mentioned above, and as the tests were carried out under vacuum to avoid any oxidation effects, the results presented below are not directly applicable to prototypical LOCA conditions. Note that in the more traditionally used Zircaloy-4 alloy, one could not "quench" the β phase by using the maximum cooling rate allowed by the facility used in this study, so that such microstructural changes were not accessible using the same temperature-time transients. Thus, no direct application of the present results to the case of Zircaloy-4 can be made.

2. Material and experimental techniques

2.1. Material

Zr–1%NbO (1 wt.% Nb, 0.14 wt.% O) thin-walled tubes were provided in the fully recrystallised state. They exhibited equiaxed α grains with an initial grain size of about 5 μm, a hardness of 180 ± 10 HV_5 (load 5 kg, holding time 15 s) with some β_{Nb} and a few (Zr, Nb, Fe) secondary phase particles. The crystallographic texture of the tubes, characterised at CEA by X-Ray diffraction, showed *c*-axes at 35° from the radial direction, in the plane normal to the tube axis, with a <11.0> direction at about 10° from the tube axis.

2.2. Experimental techniques

Uniaxial tensile creep tests were carried out along the tube axis using an electrical–mechanical testing machine equipped with a radiation furnace and a water-cooled 2000 N load cell, both inside a high vacuum chamber (vacuum better than 10^{-3} Pa). High vacuum was required in order to avoid any chemical oxidation/contamination from laboratory air. The specimen temperature was controlled using a Pt–Pt10%Rh thermocouple spot-welded onto the outer surface of the specimen. All tests were performed under load control, axial strain being monitored using a contactless laser extensometer. Phase transformations were continuously monitored using four-point resistivity measurements, which had been validated by comparison with calorimetric experiments, image analysis, equilibrium phase diagrams and kinetics calculations [3]. The various test temperatures were chosen with respect to the transformation temperatures of this alloy, i.e., about 740 °C for the $\alpha/(\alpha+\beta)$ boundary, and about 940 °C for the $(\alpha+\beta)/\beta$ phase boundary under the heating conditions that were used in this study. As there were always some retained β particles even at room temperature, low-temperature microstructures will be referred to as "near-α" microstructures throughout this paper.

After soaking for 30 min at the creep testing temperature, the load was applied with small increments, waiting for an amount of creep strain of 2% to be reached for each load step, and then applying the new value of the load within a short time (i.e., within a few seconds), and so on. This procedure allowed avoiding any primary creep stage and minimising any load history effect, as the specimen only deformed elastically upon changing the load level. The values of true axial stress and true axial strain rate were then calculated for each load step. Only true stress and true strain values are reported throughout the rest of this paper.

To investigate the effect of microstructure on creep properties, various heat treatments were applied to the specimens just before the creep tests, in the same testing machine. The heat cycles aimed at transforming the α phase fully or partially into β before creep. Four types of creep tests were thus carried out (Table 1):

(a) Isothermal tests were first carried out in the as-received condition, after "direct" heating (Fig. 1a). This is the same experimental database as that reported in [3].
(b) Isothermal tests were then carried out in the near-α temperature range on a modified microstructure (Fig. 1b). Cooling down and soaking at 575 °C for a while were carried out to ensure almost complete β to α phase transformation, α phase start and finish temperatures having been determined to be about 920 °C and 730 °C, respectively, in these conditions.
(c) Isothermal tests in the $(\alpha+\beta)$ temperature range on a modified microstructure that was fully transformed into β, but only partially transformed back into α before creep (Fig. 1c). The value of 1050 °C was chosen to ensure full α to β phase transformation.
(d) Non-isothermal creep tests under constant load (Fig. 1d) were also carried out to investigate any influence of stress on microstructural development, e.g., transformation-induced plasticity and change in phase morphology.

After creep, all specimens were cooled at −300 °C/min down to room temperature and longitudinal cross-sections were examined using light optical microscopy (LOM). In addition, some samples were subjected to heat cycle (b) interrupted by quenching after the soaking step at 575 °C for metallographic investigations. LOM observations were carried out after etching at room temperature with a (50% glycerol + 45% nitric acid + 5% hydrofluoric acid) solution (etchant 1) or a special reagent (hydrofluoric acid + colloidal silica) (etchant 2). Etchant 2 was used to reveal the α grain boundaries in microstructures heated up to less than 750 °C, which were difficult to reveal using etchant 1.

For scanning electron microscopy (SEM) observations, electrochemical etching, and then selective dissolution of the primary α phase were performed after using a special etching reagent [5]. This procedure does not affect the "prior β" phase. Both the bulk (etched) samples and extraction residues (obtained after dissolution) were examined in the SEM to assess the size and spatial distribution of phases, and in particular the three-dimensional morphology of the "prior-β" grains in the $(\alpha+\beta$ temperature range.

3. Results

3.1. Deformation-mechanism map after direct heating

First of all, it has to be mentioned that, under vacuum, the high temperature creep strength is much lower than the one measured on cladding tubes tested in a "in representative steam" environment. This is due to the strengthening effect induced by oxygen ingress into the material when the creep tests are performed under steam or any oxidising environment (see e.g., [6]). This explains the low values of stress applied here (typically, between 2 and 50 MPa).

Steady-state creep rate vs. stress and temperature data are gathered in the map of Fig. 2, together with the corresponding fraction of β phase measured using the resistivity method (see also Table 2). From these data, stress exponent, n, and activation energy, Q, were derived as in [3] by fitting parameters of the following equation to strain rate vs. stress and temperature data in the α, $(\alpha+\beta)$ and β temperature ranges:

$$\dot{\varepsilon} = \frac{A}{T}\sigma^n \exp\left(-\frac{Q}{RT}\right) \quad (1)$$

In Eq. (1), $\dot{\varepsilon}$ is the true axial strain rate, and σ is the true axial stress. Values of parameters A, n, and Q depend on the considered temperature range. They are reported in detail in [3].

Table 1
Summary of creep tests. "+" Denotes that creep tests were carried out, "–" denotes no creep test for that condition.

Type of creep test (see Fig. 1)	Creep test temperature, T_{test} (°C)														
	650	675	700	740	760	800	820	840	860	880	900	960	1000	1050	1100
(a): "Direct" heating	+	+	+	+	+	+	+	+	+	+	+	+	+	+	+
(b): T_{max} = 865 °C	+	–	+	+	+	–	–	–	–	–	–	–	–	–	–
(b): T_{max} = 1050 °C (β-heat treated alloy)	+	–	+	+	+	–	–	–	–	–	–	–	–	–	–
(b): T_{max} between 865 and 1050 °C	–	–	+	–	–	–	–	–	–	–	–	–	–	–	–
(b): T_{max} = 865 °C, various amounts of soaking time at T_{max}	–	–	+	–	–	–	–	–	–	–	–	–	–	–	–
(c): β-heat treated alloy	–	–	–	–	–	+	–	+	+	+	+	–	–	–	–
(d): Non-isothermal creep	Initial value of applied stress: 0 or 1 or 2 MPa (10 °C/min); 0 or 1 or 2 or 2.5 or 3 MPa (200 °C/min)														

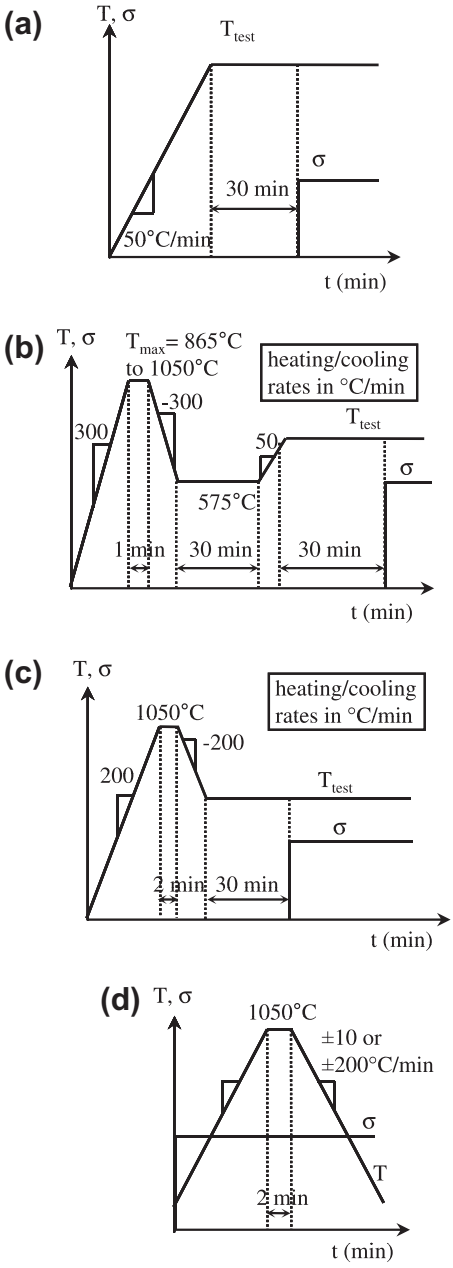

Fig. 1. Creep tests carried out in the present study. (a) Isothermal creep tests in the as-received condition ("direct heating"). (b) Isothermal creep tests of a modified microstructure in the near-α temperature range. (c) Isothermal creep tests of a modified microstructure in the (α + β) temperature range. (d) Non-isothermal creep tests under constant load.

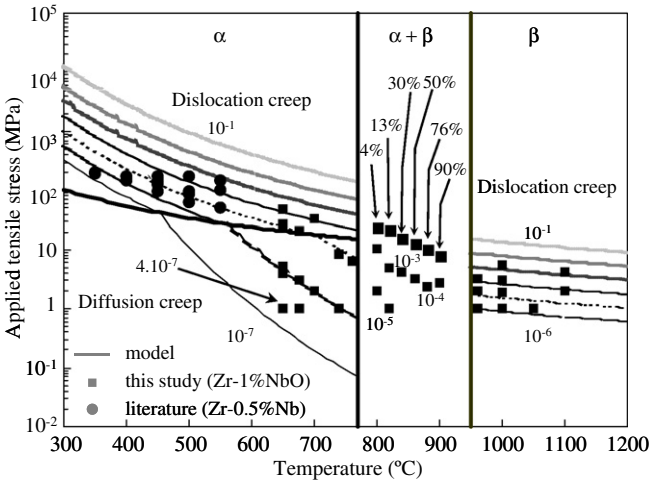

Fig. 2. Deformation-mechanism map for the Zr–1%NbO alloy under axial tension. Amounts of β phase, as measured by the resistivity method, are indicated in the (α + β) temperature range. Constant strain rate lines are plotted (in s^{-1}) for every decade. After [3] and literature data from [2].

Table 2
Amount of β phase measured using the resistivity method and by image analysis after isothermal creep tests in the (α + β) temperature range.

Type of creep test (see Fig. 1)	Measurement technique	Creep test temperature, T_{test} (°C)					
		800	820	840	860	880	900
(a): "Direct" heating	Resistivity measurements	4	13	30	50	76	90
(a): "Direct" heating	Image analysis after rapid cooling	3	9	27	45	68	81
(c): Fully-β-heat treated and partially transformed during cooling before creep	Resistivity measurements	6	No test	22	36	66	78

Two creep regimes were found in the near-α domain. Only one regime corresponding to the higher stress exponent was found for the β temperature range (stress exponent of about 4.3, Fig. 3). Only one regime corresponding to the lower stress exponent was found for the (α + β) temperature range (stress exponent of about 1.4, Fig. 4). The corresponding activation energy was found to be consistent with literature data on zirconium [1,3]. According to [1], the low-stress creep regime will be denoted here as the "diffusion" creep regime. The transition between the two regimes occurs for a true axial stress of about 10 MPa. Surprisingly, for applied stresses

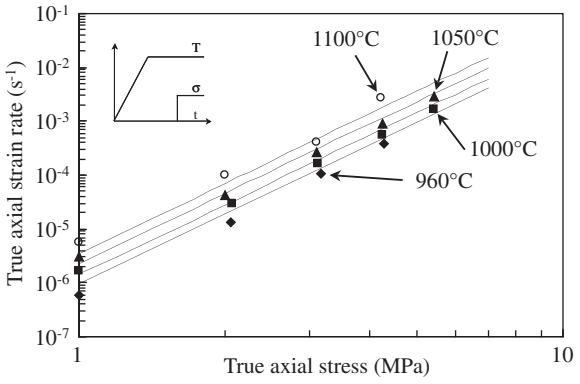

Fig. 3. Creep curves in the single β phase temperature range after direct heating.

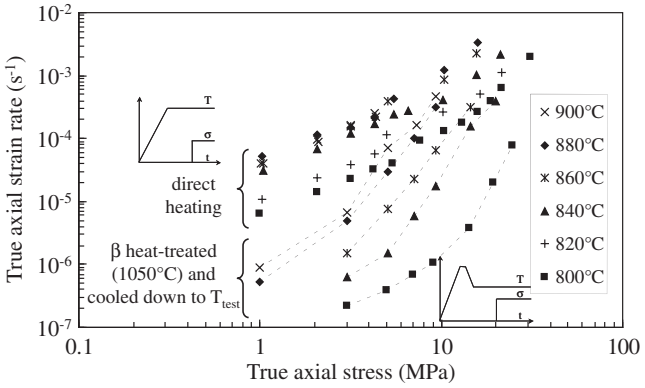

Fig. 4. Creep curves of specimens tested in the $(\alpha+\beta)$ temperature range after direct heating and after a β heat treatment (cycling up to 1050 °C).

lower than about 4 MPa, the two-phase material shows a higher creep strain rate than does the 100%-β material at higher temperature. Further tests in the $(\alpha+\beta)$ temperature range were thus carried out to clarify this point.

3.2. Microstructural effects on the creep behaviour in the $(\alpha+\beta)$ temperature range

Creep properties in the $(\alpha+\beta)$ temperature range (i.e., for at least 5% of each phase during the creep test) were investigated for two metallurgical states: in the as-received condition ("direct heating") and after a full β heat cycle (Type (c)-creep tests). This allows (i) investigating the influence of microstructure on steady-state creep, and (ii) building a metallurgical tool to further test new model microstructures in the near-α range (see next section).

There is a huge effect of microstructure on the steady-state creep in the $(\alpha+\beta)$ temperature range (Fig. 4, Table 3), along with a significant modification of phase morphology. Thanks to the "special etching" procedure, it was possible to compare the traditional two-dimensional (2D) observations (from polished samples) with a three-dimensional (3D) view (extracted residues) of the "prior β" phase, which was considered to be β phase at the creep test temperature. This was very interesting since spatial "percolation" – or not – of the β phase was expected to play a major role on the overall macroscopic creep of the two-phase material. After the "direct heating" creep tests, and according to the testing temperature, equiaxed α grains were surrounded by grain boundary β films (800 °C, Fig. 5a) or by more equiaxed, connected β grains (860 and 880 °C, Fig. 5 b and c). In the microstructure modified by the β heat

Table 3
Creep rates measured after various heat treatments normalised by creep rates measured after direct heating (for the same true stress). "–" Means that no data was available close to the considered applied stress; (a) means a soaking time of 30 min (instead of 1 min) at T_{max} during the heat treatment.

Type of creep test (see Fig. 1)	T_{test}	Normalised creep rate for σ = 4 MPa	Normalised creep rate for σ = 21 MPa
(b) (T_{max} = 865 °C)	650 °C	1.3	1.8
	700 °C	2.1	2.5
	700 °C (a)	1.4*	2.0
	760 °C	2.0	–
(b) (T_{max} = 885 °C)	700 °C	2.5*	2.8
(b) (T_{max} = 915 °C)	700 °C	6.0×10^{-1}*	7.9×10^{-1}
(b) (T_{max} = 930 °C)	700 °C	2.0×10^{-1}	4.0×10^{-1}
(b) (T_{max} = 1050 °C)	650 °C	1.7×10^{-3}	2.8×10^{-2}*
	700 °C	3.7×10^{-3}	2.8×10^{-2}
	740 °C	2.2×10^{-3}	–
	760 °C	1.2×10^{-3}	–
(c)	800 °C	9.4×10^{-3}*	4.9×10^{-3}*
	840 °C	5.9×10^{-3}*	1.9×10^{-1}*
	860 °C	1.7×10^{-2}*	–
	880 °C	6.2×10^{-2}*	–
	900 °C	1.2×10^{-1}*	–

* Denotes a value that was calculated by interpolation of creep data by using Eq. (1) (correlation ratio higher than 0.95).

treatment, large colonies of α crystals, which were shown using serial sectioning to be plate-shaped, appeared surrounded by huge grains of the β matrix (Fig. 6). Thus, both grain size and morphology changed as a result of the β heat cycle, making the low stress regime even disappear.

While a stress exponent of nearly 1 was found up to a creep strain rate of 10^{-4} s^{-1} after direct heating, a higher stress exponent was found even for creep strain rates as low as 10^{-7} s^{-1} after the β heat treatment. The effect of temperature on the creep strain rate was not significant for creep temperatures between 860 and 900 °C after direct heating; it was more pronounced throughout the whole $(\alpha+\beta)$ temperature range after the β heat treatment. The effect of microstructure tends to be lower in the higher stress creep regime. It could thus be due to a strong modification of the material flow behaviour in the lower stress creep regime.

3.3. Microstructural effects on the creep behaviour in the near-α temperature range

To study the effect of microstructure on creep flow of the near-α material, heat treatment (b) involving either partial or total transformation upon the first heating from α to β, followed by reverse transformation to form various amounts of "prior β" before creep, was used. Two temperatures were first chosen: 1050 °C (fully "prior β") and 865 °C (around 50% equiaxed α + 50% "prior β"). Thus, two near-α microstructures were tested in creep: the as-received one (equiaxed α grains) and the heat-treated one (equiaxed α grains + "prior β").

The effect of such heat cycle up to 865 °C is very limited (Fig. 7a, Table 3): it induced a slight (two-fold) acceleration of creep. In fact, "prior β" colonies exhibited intensive recovery during the creep test, leading to a nearly equiaxed α microstructure close to that obtained after direct heating in the same conditions (Fig. 7b and c).

On the contrary, a strong effect of the heat cycle up to 1050 °C was found (Fig. 8, Table 3). For creep tests at 650, 700 and 760 °C, two specimens were used: one for stress levels from 2 to 10 MPa,

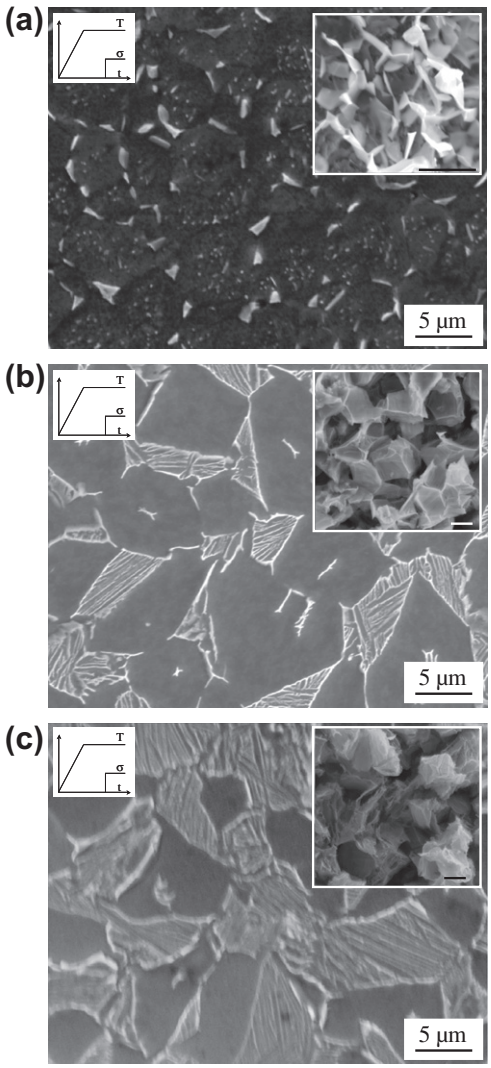

Fig. 5. Scanning electron micrographs of specimens crept after direct heating up to (a) 800 °C (4% β), (b) 860 °C (50% β) and (c) 880 °C (76% β). Inlets show the 3-D morphology of, "prior β" phase as observed from extraction residues (the scale bar in inlets stands for 5 μm).

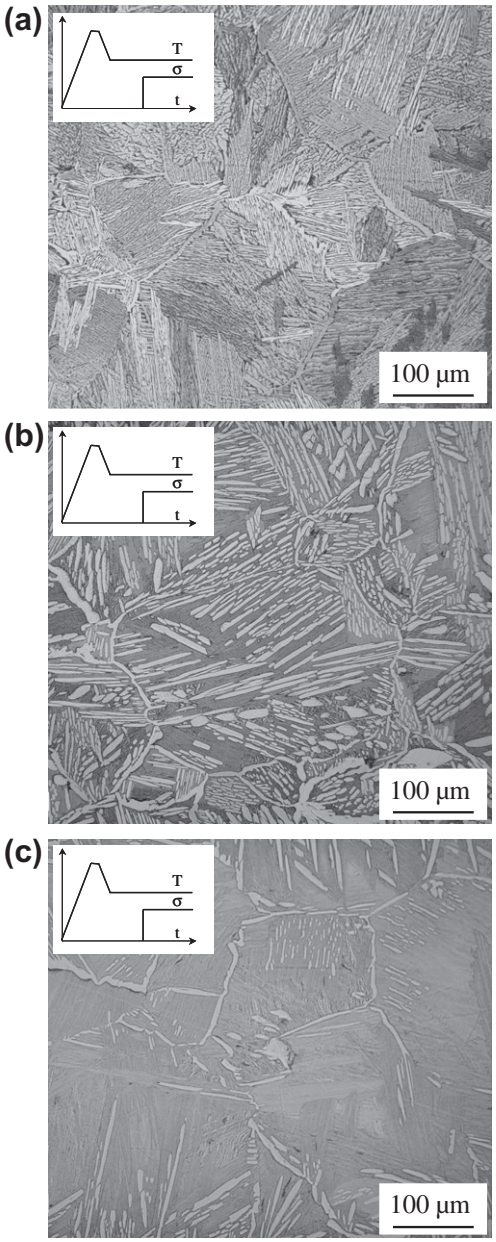

Fig. 6. Light optical micrographs of specimens crept after type (c)-creep tests, for T_{test} = (a) 800 °C (6% β), (b) 860 °C (36% β) and (c) 880 °C (66% β). Colonies of α phase (transformed during cooling, but before creep) are in light grey, while the remaining β phase transformed into a more acicular product during cooling (in darker grey).

and another one for stress levels from 10 to 50 MPa. The two specimens yielded different creep results under a true stress of 10 MPa. First, it was checked that this effect was not due to a drift of load cell measurements. It could possibly be due to a slight sensitivity to the loading history at 10 MPa, because a continuous curve was obtained using a single specimen at 740 °C. It seems to only affect strain rate measurements at 10 (and possibly 20) MPa in the specimen tested for higher stress levels and will not be further discussed here. Nevertheless, the heat treatment led in any case to a decrease in creep strain rate by more than one order of magnitude with respect to the "direct heating" case. The marked decrease in creep strain rate for low stress levels was again attributed to some mechanism inhibiting diffusion creep. This effect tended to disappear under higher stresses. A stable "prior-β" colony-shaped near-α microstructure was produced by this heating cycle (Fig. 8c), with retained β films enriched in Nb. The Nb content of these films was measured from extractive replicas using energy dispersive spectrometry in the SEM, yielding values ranging between 13 and 16 wt.%.

To explore intermediate microstructures, heat cycles with various values of T_{max} ranging between 865 and 1050 °C were applied, leading to various amounts of "prior β" colonies and thus to various creep behaviours (Fig. 9, Table 4). As will be shown below, no significant microstructural evolution was found during creep, so that the amount of β phase at $T = T_{max}$ was deduced from continuous potential drop measurements during a heating cycle at the same heating rate. For former β grains smaller than about 10–15 μm (up to T_{max} = 885 °C, 80% β), the maximum cooling rate of the experimental device was not high enough to produce colony-shaped "prior β" colonies that would be stable against annealing at 700 °C (Fig. 9b and c). For β grains larger than 10–15 μm (T_{max} > 885 °C), "prior β" colonies were much more stable at 700 °C and provided increasing resistance to diffusion creep with increasing T_{max}. Thus, associated with the higher β grain size, the colony-shaped microstructure is intimately related to the resistance to diffusion creep, although the specific area of α/β interphase interfaces is very high for both kinds of microstructures.

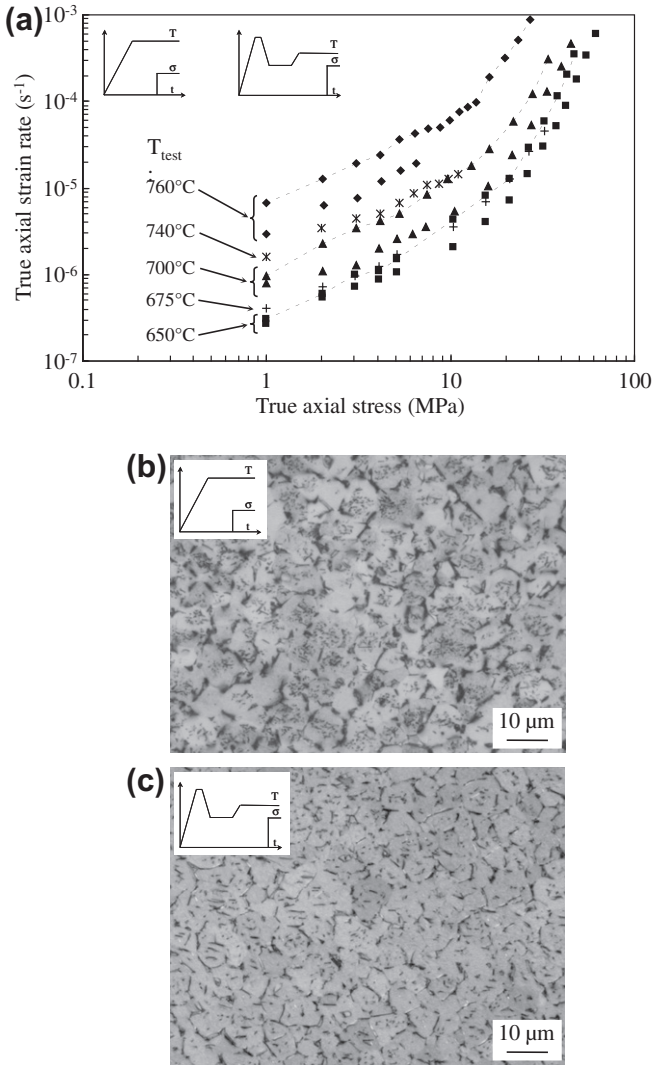

Fig. 7. Effect of prior heat treatment up to 865 °C (around 50% β). (a) Creep curves in the near-α domain (dashed lines for heat-cycled specimens, no line for direct-heated specimens, one symbol per test temperature). Light optical micrographs of samples crept at 760 °C after (b) direct heating and (c) heat cycling up to 865 °C.

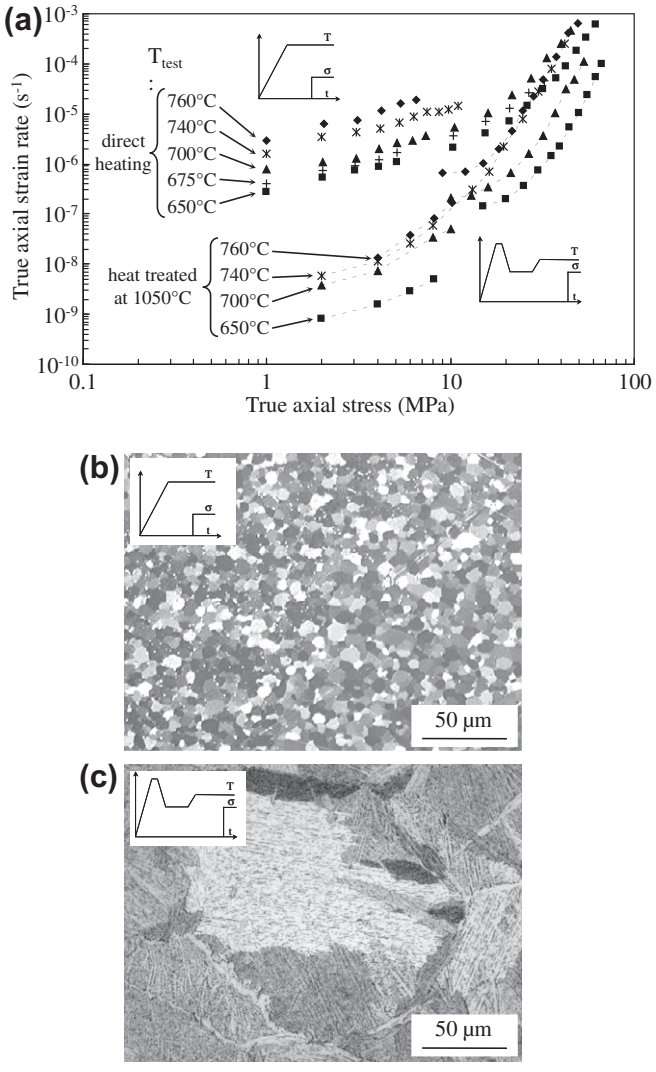

Fig. 8. Effect of prior heat treatment up to 1050 °C (100% β). (a) Creep curves in the near-α domain; (b and c) light optical micrographs of specimens tested at 650 °C after (b) direct heating + creep and (c) a type (b)-creep test.

3.4. Reverse coupling: which effect of applied stress on microstructural evolution?

The previous sections showed a strong effect of microstructure on creep flow properties. This section addresses the reverse question, i.e., the possible effect of stress on the microstructural evolution during creep. As shown below, this effect seems to be negligible for the experimental conditions investigated in this study.

First, no evolution of microstructure was detected after creep, compared to a stress-free heat treatment in the same conditions. The only evolution that was noticed after creep (with respect to the same heat cycle, but interrupted just before applying the load) was an anneal of the small "prior-β" grains in specimens treated at 865–885 °C and crept at around 700 °C, as mentioned before. No other significant change was noticed using light optical and SEM imaging, even in the ($\alpha + \beta$) temperature range. Soaking for 30 min at the creep test temperature yielded a stable (although out of equilibrium) microstructure, which did not further significantly evolve during creep. This was confirmed by both resistivity measurements (after having subtracted the contribution of deformation to the increase in the specimen resistance, Fig. 10) and image analysis after cooling down to room temperature (Table 2). The small difference between the two sets of results in Table 2 (resistivity vs. image analysis measurements) was attributed to experimental uncertainty, due to some possible growth of the α phase during cooling. This effect could lead to a slight overestimation of the amount of α phase by the image analysis technique because metallographic pictures could only be taken at room temperature.

To further assess any history effect due to microstructural evolution, non-isothermal creep tests were analysed according to the creep behaviour already identified after "direct heating" creep tests, and after cooling from 1050 °C (type (c) cycles). By considering the experimental curves (Fig. 11) and subtracting the contribution of creep as calculated using small temperature increments (unified flow rule given by Eq. (1) for single-phase domains, one flow rule per temperature in the ($\alpha + \beta$ domain), it was shown that no transformation-induced plasticity higher than about 0.2% (the detection limit with the experimental facility used here) could be evidenced in this alloy, even during the formation of the colony microstructure. The much higher strains measured at 10 °C/min, as well as asymmetry between heating and cooling curves could be fully attributed to the already evidenced strong microstructural

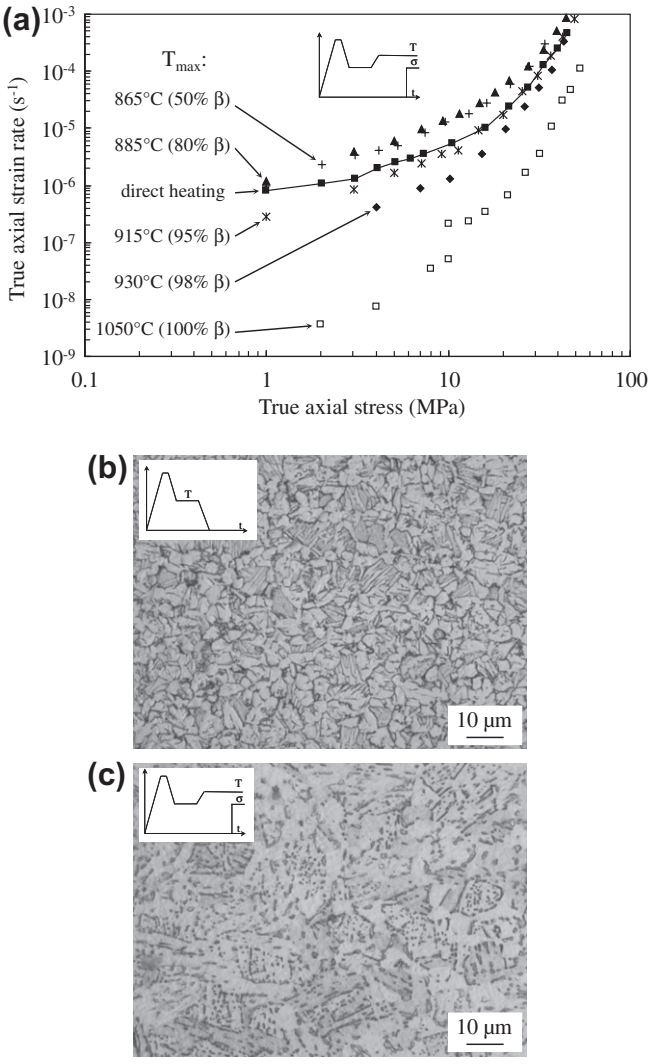

Fig. 9. Effect of maximum temperature, T_{max}, on type (b)-creep test results. (a) Creep curves at 700 °C; (b and c) light optical micrographs of samples heat-treated up to 930 °C, cooled down to 575 °C and (b) cooled down to room temperature, (c) creep tested at 700 °C.

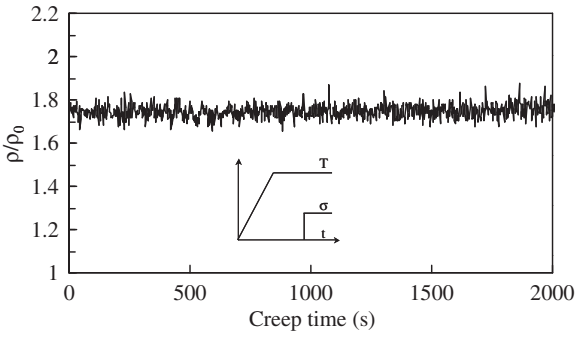

Fig. 10. Evolution of the specimen resistivity during a creep test after direct heating up to 800 °C and stabilisation of temperature (soaking). ρ_0 is the resistivity of the specimen prior to heating.

effects on creep flow. Unlike Zircaloy-4 [7], the investigated Zr–1%NbO alloy did not show any transformation-induced (visco)plasticity. Last but not least, stress did not influence the transformation kinetics during heating beyond the detection limit (i.e., by a shift of at least 10 °C).

4. Discussion

4.1. General trends of the creep behaviour of the Zr–1%NbO alloy

The effect of microstructure on creep in the near-α temperature range is similar to what was found with a Ti6242–Si alloy [8] after an anneal in the (α + β) temperature range leading to a volume fraction of primary α phase between a few % and 53%; a three-fold increase in both primary and steady-state creep strain rates was found in the material containing the highest amount of primary α. This effect was attributed to an interaction between phase morphology (e.g., banding of primary α phase), and creep of retained β films, which was, in addition, strongly influenced by Ni impurity (see also [9]). Similar results for creep temperatures between 480 and 565 °C were reported for both Ti6242–Si and IMI834 near-α titanium alloys, with the same order of magnitude (by a factor from 2 to less than 5) for the effect of microstructure on the creep strain rate [10–12]. In addition, a significant influence of microstructure was found for powder-metallurgy Ti1100 and Ti6242

Table 4
Microstructural evolution and creep flow at 700 °C of specimens cycled at various peak temperatures before the creep test.

Maximum temperature (1 min dwell) (creep test of type (b))	865 °C	885 °C	915 °C	930 °C	1050 °C
% β at T_{max} (resistivity measurements during continuous heating)	50%	80%	95%	98%	100%
Creep rate at 4 MPa normalised by that measured after direct heating	2.0	2.5	0.60	0.20	0.00036
Microstructure after cooling down to 575 °C	Equiaxed α grains (5 μm) + inter- and intra-granular retained (Nb-enriched) β films	Equiaxed α grains (5 μm) + inter- and intra-granular retained β films + some equiaxed "prior-β" grains (5 μm)	Equiaxed α grains (5 μm) + equiaxed "prior-β" grains (~10–15 μm)	Equiaxed α grains (5 μm) + equiaxed "prior-β" grains (~20 μm)	Huge β grains (>300 μm) transformed into basket weave α colonies during cooling
Further evolution after creep at 700 °C	Annealing of "prior-β" grains	Annealing of "prior-β" grains	Spheroidisation of intra-granular retained β films into aligned particles	Spheroidisation of intra-granular retained β films into aligned particles	Some spheroidisation of intra-granular retained β into aligned particles

alloys crept in the near-α temperature range: a colony microstructure with low angle boundaries showed much higher creep resistance than a basketweave microstructure with a high density of high-angle boundaries [13].

In the present study, however, the microstructural effect is much stronger for stress levels lower than 10 MPa. It could probably not be only attributed to chemical changes in the α phase, as was the case for creep at 400 °C of a similar Zr–1%NbO alloy [14]. Oxygen is known to markedly partition between α and β phases, even for cooling rates that are much higher than those used in the present study [15], so that no significant difference in the oxygen content of the α phase is expected between the various near-α microstructures. Although the role of partitioning of niobium remains to be clarified, such a strong effect of microstructure cannot be explained only by a change in chemistry of α and β phases, respectively.

The creep behaviour of the material in the near-α temperature range (after "direct heating", type (a) cycles) classically shows the two power-law creep regimes expected from this alloy family. However, surprisingly, the low stress exponent, diffusion creep regime was not evidenced for the fully β temperature range. This could be due to (i) resistance of β grain boundaries to Coble-type diffusion creep and (ii) to a low density of β grain boundaries. From metallographic observations, as soon as the α phase disappeared, β grain growth occurred, leading to coarse β grains (>100–200 μm in size) and thus to a low density of grain boundaries. The same kind of results was already obtained in polycrystalline, (probably) coarse-grained β-titanium, with a power-law exponent of about 4.2 for a wide range of creep strain rates (10^{-7}–10^{2} s^{-1}), of applied stresses (0.5–50 MPa) and of test temperatures (900–1300 °C) [16]. It was also attributed to the coarse grain size of fully β titanium alloys at high temperature, allowing dislocation-controlled creep to be the dominant deformation mechanism for the loading conditions experimentally tested. In the case of Zr–1%NbO-type alloys, this possible effect of the β grain size is being characterised and confirmed in ongoing work [17,18].

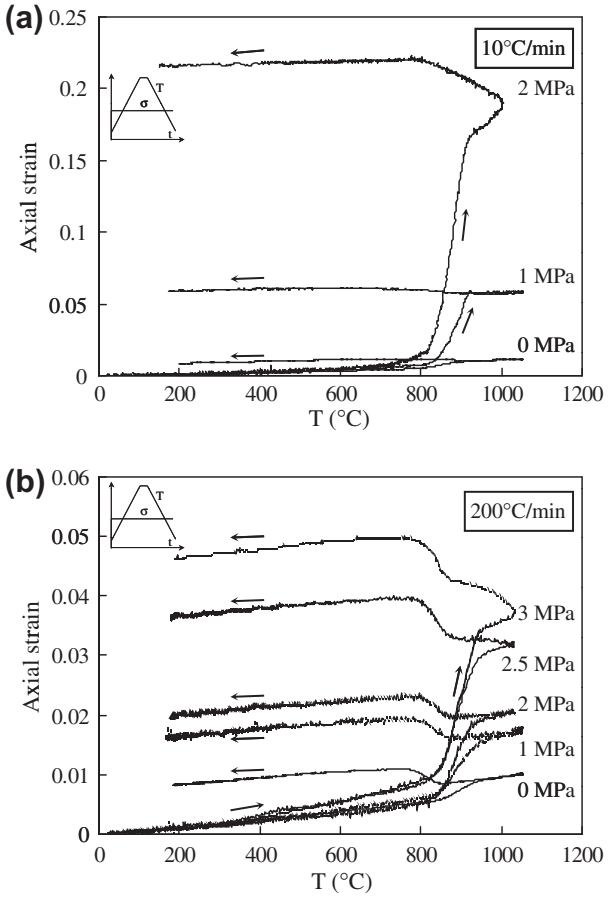

Fig. 11. Dilatometry curves obtained for various values of the nominal stress (indicated on the right of corresponding curves). Arrows pointing to the right and to the left indicate the heating and cooling parts of the curves, respectively.

4.2. Diffusion creep flow in the ($\alpha + \beta$) range after direct heating

After direct heating, the two-phase alloy is very sensitive to diffusion creep flow. This could be due to several reasons: (i) a high mobility of α/β interphase interfaces; (ii) the small size of both α and β grains in the two-phase temperature range, and (iii) local stress or strain concentrations due to phase morphology. Hypothesis (iii) alone was quickly eliminated: even after crystal viscoplasticity finite element calculation of representative ($\alpha + \beta$) aggregates [19], the creep strain rate of ($\alpha + \beta$) material should always range between those extrapolated from single-phase domains, as expected in continuum mechanics homogenisation theory. No significant damage was detected at α/β interphase interfaces (in fact, only one specimen fractured at the end of a test), even after more than 10% of strain, which indicates that surface mobility was not the only explanation, although the "percolation" threshold of the β phase (and thus of α/β interphase interfaces) after direct heating, at 840 °C, seemed to play a role in the creep flow at low stresses. There is a need to assess the effects of α and β grain size on creep, as diffusion creep is very sensitive to the grain size. The same effect was thought to play a role in the reverse temperature dependence of low-stress (1–4 MPa) creep flow ($n \sim 2$) of a Ti–6Al-4 V alloy in the ($\alpha + \beta$) $\Leftrightarrow$ β transition temperature range [20]. Work on this issue is currently in progress in a Zr–1%NbO-type alloy [18,19].

The strong effect of microstructure on the creep flow behaviour in the ($\alpha + \beta$) two-phase temperature range explains the asymmetric dilatometric behaviour of the Zr–1%NbO alloy between heating and cooling. The curves of Fig. 11 obtained at 10 °C/min closely resemble those obtained by Leriche et al. [20] with a Ti–6Al-4 V alloy under low stress (typically, 7 MPa). Leriche et al. also evidenced a strain rate much lower on cooling than on heating in the phase transition temperature range, from which the authors concluded to a different transformation-induced plasticity effect on heating vs. on cooling. The results of the present study strongly suggest that such experimental data must be processed by subtracting creep deformation in the relevant temperature range *and for the relevant metallurgical state* (e.g., on heating vs. on cooling) before concluding to a transformation-induced plasticity effect, or even to a superplasticity effect in Zr-based alloys, and probably also on Ti-based alloys [21–23].

5. Conclusions

The present investigation of the microstructural influence on the creep flow of a Zr–1%NbO alloy led to the following results:

- A very strong effect of microstructure (grain size and shape) on the creep flow behaviour was detected in the near-α and ($\alpha + \beta$) temperature ranges, at least for stress levels lower than about 10 $\sim$ 20 MPa. An equiaxed, fine-grained microstructure promoted diffusion creep, whereas a "α colony" microstructure (i.e., transformed β with a plate-shaped or basketweave morphology) strongly inhibited diffusion creep, leading to a drop in creep flow at low stresses.

- No effect of applied stress (or, conversely, of creep flow) was detected on phase morphology, transformation kinetics and amount of transformed phases. Apart from some annealing of smallest colony-shaped α crystals at 700–760 °C, no microstructural evolution was evidenced during the creep tests. No transformation-induced viscoplasticity was detected during heat cycles under a stress up to 3 MPa, once the contribution of creep deformation was thoroughly subtracted from the total strain vs. time curves.
- The present results help understanding the striking behaviour of the Zr–1%NbO alloy in the $(\alpha + \beta)$ temperature range. The most probable underlying mechanisms are high diffusion kinetics along α/β interphase interfaces and a strong grain size effect. These are currently under investigation.

Acknowledgements

Technical support from Michel Rousselot and Julie Heurtel (Centre des Matériaux) and from Stéphane Urvoy and Thomas Guilbert (CEA) is gratefully acknowledged.

References

[1] P.M. Sargent, M.F. Ashby, Scr. Metall. 16 (1982) 1415–1422.
[2] M. Pahutová, J. Čadek, V. Černý, J. Nucl. Mater. 61 (1976) 285–296.
[3] D. Kaddour, S. Fréchinet, A.F. Gourgues, J.C. Brachet, L. Portier, A. Pineau, Scr. Mater. 51 (2004) 515–519.
[4] I. Charit, K.L. Murty, J. Nucl. Mater. 374 (2008) 354–363.
[5] C. Toffolon, J.-C. Brachet, G. Jago, J. Nucl. Mater. 305 (2002) 224–231.
[6] T. Forgeron, J.C. Brachet, F. Barcelo, A. Castaing, J. Hivroz, J.P. Mardon, C. Bernaudat, ASTM STP 1354 (2000) 256–278.
[7] S. Fréchinet, A.F. Gourgues, T. Forgeron, J.C. Brachet, A. Pineau, Transformation induced plasticity in zircaloy 4, in: D. Miannay, P. Costa, D. François, A. Pineau (Eds.), Proceedings EUROMAT 2000, Elsevier Science, Amsterdam, 2000, pp. 829–834.
[8] K.E. Thiehsen, M.E. Kassner, J. Pollard, D.R. Hiatt, B.M. Bristow, Metall. Trans. 24A (1993) 1819–1826.
[9] R.W. Hayes, G.B. Viswanathan, M.J. Mills, Acta Mater. 50 (2002) 4953–4963.
[10] S.R. Seagle, G.S. Hall, H.B. Bomberger, Met. Eng. Quart. 15 (1975) 48–54.
[11] P.J. Bania, J.A. Hall, Creep studies of Ti6242–Si alloy, in: G. Lütjering, U. Zwicker, W. Bunk (Eds.), Proceedings Titanium Science and Technology 1984, Deutsche Gesellschaft für Metallkunde, Oberursel, Germany, 1985, pp. 2371–2378.
[12] H. Mishra, P. Ghosal, T.K. Nandy, P.K. Sagar, Mater. Sci. Eng. A399 (2005) 222–231.
[13] M. Hagiwara, S. Emura, Mater. Sci. Eng. A352 (2003) 85–92.
[14] R. Brenner, J.L. Béchade, O. Castelnau, B. Bacroix, J. Nucl. Mater. 305 (2002) 175–186.
[15] A. Stern, J.C. Brachet, V. Maillot, D. Hamon, F. Barcelo, S. Poissonnet, A. Pineau, J.P. Mardon, A. Lesbros, J. ASTM Int. 5 (4) (2008) JAI101119.
[16] C. Schuh, D.C. Dunand, Scr. Mater. 45 (2001) 1415–1421.
[17] N. Richard, Effect of grain size on high-temperature isothermal creep behaviour of a Zr–1%Nb (O) alloy, Master dissertation, MINES ParisTech, 2008 (in French).
[18] G. Trego, Experimental study and modelling of creep in a zirconium alloy in the $(\alpha + \beta)$ temperature range, Ph.D. dissertation, MINES ParisTech, France, to be defended, 2011 (in French).
[19] D. Kaddour, Isothermal and non-isothermal creep of a Zr–1%NbO alloy in the single α and β phase, and in the two-phase $(\alpha + \beta)$ temperature ranges, Ph.D. dissertation, Ecole des Mines de Paris, Paris, France, 2004, <http://pastel.paristech.org/1477/> (in French).
[20] D. Leriche, E. Gautier, A. Simon, Mechanical behaviour of a forged and a HIP'ed TA6V4 alloy in the phase transformation $\alpha + \beta \Leftrightarrow \beta$ temperature range, in: P. Lacombe, R. Tricot, G. Béranger (Eds.), Proceedings 6th World Conference on Titanium, vol. 1, Les Editions de Physique, Les Ulis, France, 1988, pp. 163–168.
[21] P. Zwigl, D.C. Dunand, Metall. Mater. Trans. 29A (1998) 2571–2582.
[22] H.J. Gonzalez, D.C. Dunand, J. Mater. Eng. Perform. 13 (2004) 665–669.
[23] H. Choe, C.A. Schuh, D.C. Dunand, J. Appl. Phys. 103 (2008) 103518-1–103518-9.